

PROCEEDINGS OF SPIE

[SPIDigitalLibrary.org/conference-proceedings-of-spie](https://spiedigitallibrary.org/conference-proceedings-of-spie)

Residual flatness error correction in three-dimensional imaging confocal microscopes

Carlos Bermudez, André Felgner, Pol Martinez, Aitor Matilla, Cristina Cadevall, et al.

Carlos Bermudez, André Felgner, Pol Martinez, Aitor Matilla, Cristina Cadevall, Roger Artigas, "Residual flatness error correction in three-dimensional imaging confocal microscopes," Proc. SPIE 10678, Optical Micro- and Nanometrology VII, 106780M (24 May 2018); doi: 10.1117/12.2306903

SPIE.

Event: SPIE Photonics Europe, 2018, Strasbourg, France

Residual Flatness Error correction in three dimensional Imaging Confocal Microscopes

Carlos Bermudez*^a, André Felgner^b, Pol Martinez^a, Aitor Matilla^a, Cristina Cadevall^a, and Roger Artigas^a

^aSensofar Tech SL, Barcelona, Spain; ^bPhysikalisch-Technische Bundesanstalt (PTB), Braunschweig, Germany

ABSTRACT

Imaging Confocal Microscopes (ICM) are highly used for the assessment of three-dimensional measurement of technical surfaces. The benefit of an ICM in comparison to an interferometer is the use of high numerical aperture microscope objectives, which allows retrieving signal from high slope regions of a surface. When measuring a flat sample, such as a high-quality mirror, all ICM's show a complex shape of low frequencies instead of a uniform flat result. Such shape, obtained from a $\lambda/10$, Sa < 0.5 nm calibration mirror is used as a reference for being subtracted from all the measurements, according to ISO 25178-607. This is true and valid only for those surfaces that have small slopes. When measuring surfaces with varying local slopes or tilted with respect to the calibration, the flatness error calibration is no longer valid, leaving what is called the residual flatness error.

In this paper we show that the residual flatness error on a reference sphere measured with a 10X can make the measurement of the radius to have up to 10% error. We analyzed the sources that generate this effect and proposed a method to correct it: we measured a tilted mirror with several angles and characterized the flatness error as a function of the distance to the optical axis, and the tilt angle. New measurements take into account such characterization by assessing the local slopes. We tested the method on calibrated reference spheres and proved to provide correct measurements. We also analyzed this behavior in Laser Scan as well on Microdisplay Scan confocal microscopes.

Keywords: Imaging systems, Confocal Microscopy, Metrology, Surface measurements, Calibration

1. INTRODUCTION

Imaging confocal microscopes (ICM) are widely used for areal measurements thanks to its good height resolution and the capability to measure high local slopes. Other technologies such as Coherence Scanning Interferometry (CSI) and Focus Variation (FV) are also widely used for the measurement of technical surfaces [1]. Interferometry provides the highest vertical resolution independently of the numerical aperture of the objective, but it has the drawback of being highly sensitive to vibrations and requires a dense Z scan to extract the areal information. When measuring a flat sample, such as a high-quality mirror, all ICM's show a complex shape of low frequencies instead of a uniform flat result. ISO 25178-607 [2] states that a $\lambda/10$ calibration mirror with less than 0.5 nm Sa roughness should be measured, and the result topography used as a reference of the flatness error calibration to be subsequently subtracted from the following measures [3]. This is true and valid only for those surfaces that have small slopes. Nevertheless, when the object imaged through the microscope is tilted, the effective numerical aperture changes along the pupil of the confocal microscope objective, and the field curvature changes. This makes the flatness error to be no longer valid, leaving an additional error called residual flatness error. The amplitude of this error is proportional to the local slope of the surface.

When measuring cylindrical surfaces, an optical profiler cannot get the full topography along a full revolution [4]. The sample has to be fixed on a rotational stage, and several topographies have to be acquired and stitched at different rotation angles. With this method, the residual flatness error is particularly harmful, as stitching will not be accurate due to curvatures mismatch.

Flatness error is a well-known limitation of optical 3D profilers. Although previous study on ICM [5] and CSI [6] has been made, we propose, for the first time, a characterization and correction method that applies to confocal 3D profilers.

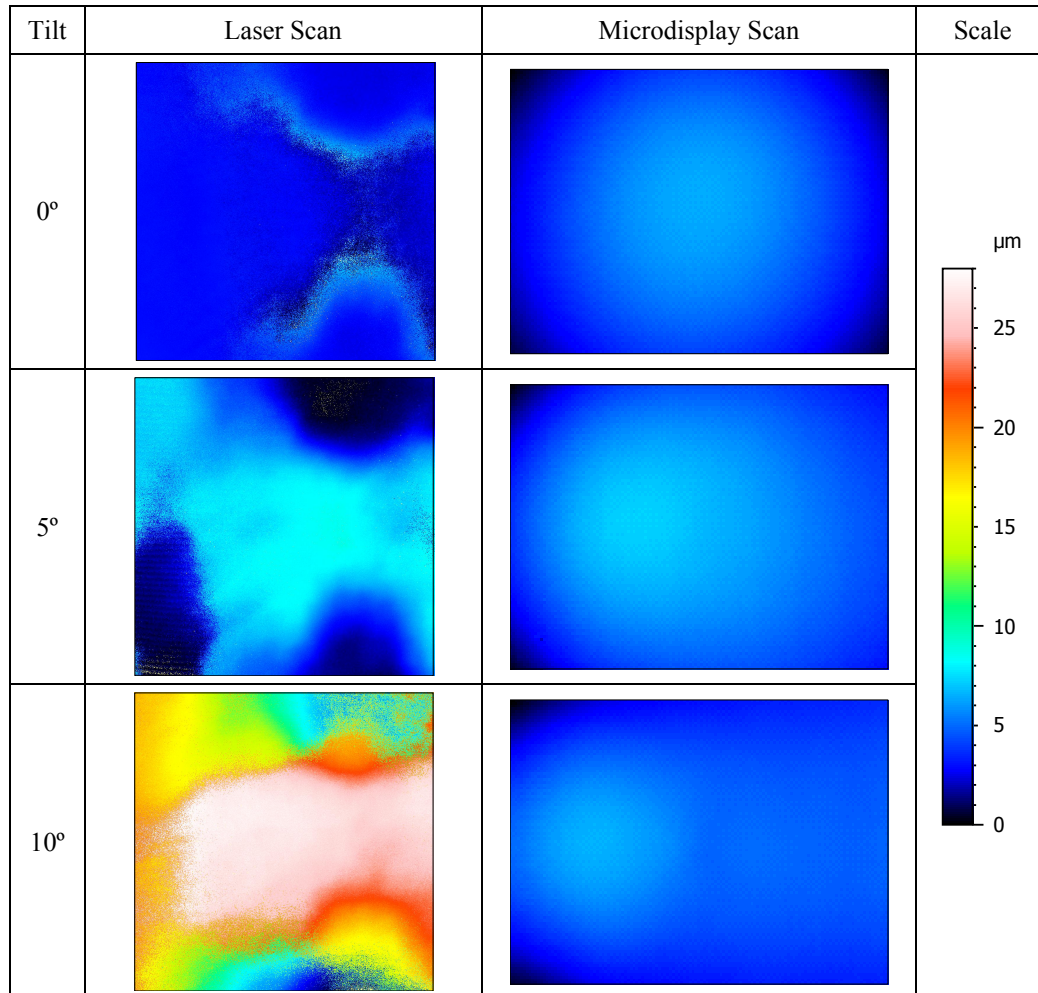
[*bermudez@sensofar.com](mailto:bermudez@sensofar.com);

phone +34 93 700 14 92;

www.sensofar.com

In order to prove that this behavior is related to optical parameters, we have studied two different Imaging Confocal Microscope approaches: a Laser Scan and Microdisplay Scan [2]. We have measured a flat mirror with increasing tilt from 0° to 10° with a 10X 0.3NA objective. At 0° , the flatness error matches the field curvature of an optical system with an object perpendicular to the optical axis whereas with a tilt the form loses its symmetry of revolution (Table 1).

Table 1. Flatness error of a mirror with different tilt angles for each type of ICM, surface is leveled according to the angle.



Apart from losing the symmetry of revolution with increasing angles, peak to valley value is completely different between the two analyzed confocal approaches, as can be observed in Figure 1.

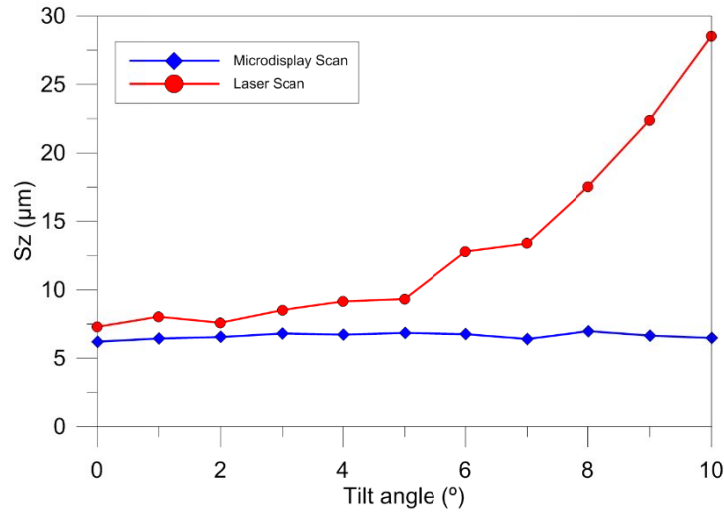


Figure 1. Sz of the residual flatness error topography with different slopes, for two different confocal microscopes.

A simulation of the Petzval field curvature was compared with the obtained measurements. Due to the unavailable optical design of the used microscope objectives, we performed the ray tracing with a 0.5X tube lens and a paraxial 10X 0.3NA microscope objective (Fig. 2a). It can be observed from such comparison (Fig. 2b and 2c) that the measurements follow the simulated values, taking into account that the simulated objective is dissimilar to the real one.

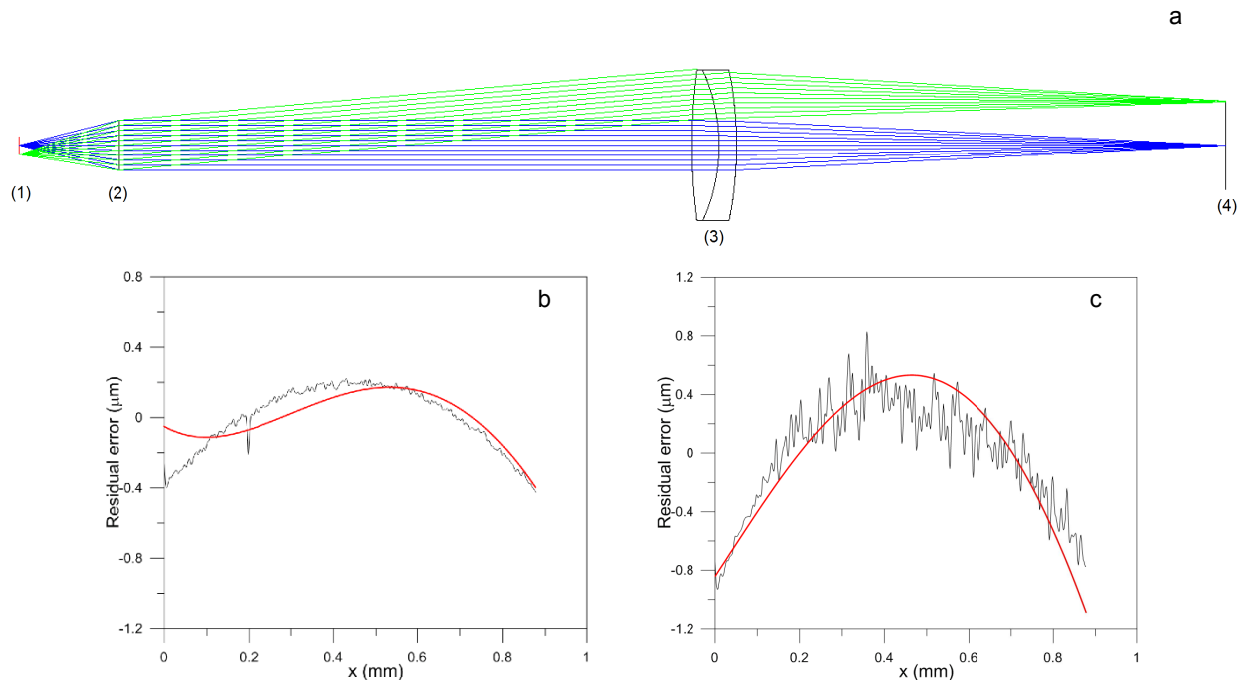


Figure 2. (a) Optical simulation of the imaging path of the confocal microscope (1) object, (2) paraxial 10X microscope objective, (3) tube lens, (4) image plane. Simulated (red) and measured (black) residual flatness error of the object at (b) 0° tilt, (c) 10° tilt. 0mm distance corresponds to the optical axis.

The rest of the paper is organized as follows: on section 2, the method to characterize, model and correct the flatness error according to the local slope is presented. Section 3 shows the results on real measurements implementing the explored method. On section 4 the results and further work is discussed whereas section 5 presents the conclusions.

2. METHOD

In any confocal microscope profiler, the flatness error is characterized by measuring a flat mirror perpendicular to the optical axis, and subsequently subtracting its topography for further measurements. The method we are proposing is to follow a similar concept, but with the characterization of the flatness error as a function of the slope and the distance to the optical axis. The steps to accomplish such method are the following:

1. Measure a set of topographies with variable tilt along the X direction and subtract the profile starting from the optical axis to the edge of the measurement.
2. Remove the tilt and construct a 3D surface with the distance to the optical center in the X-axis, the tilt angle on the Y-axis, and the flatness error on the Z-axis. Find a mathematical function that best fits the previous surface.
3. On a new measurement, calculate the local slope and the distance to the optical center for all the pixels, and subsequently subtract the error.

2.1 Flatness error characterization

The first step to characterize the flatness error is to measure a flat mirror with different tilts in the X direction, including positive and negative angles. The center X profile is extracted and after removing the tilted plane, some symmetry is observed: the residual profile of certain angle is symmetric respect to the center compared to the same residual profile with the negative angle as shown in Figure 3.

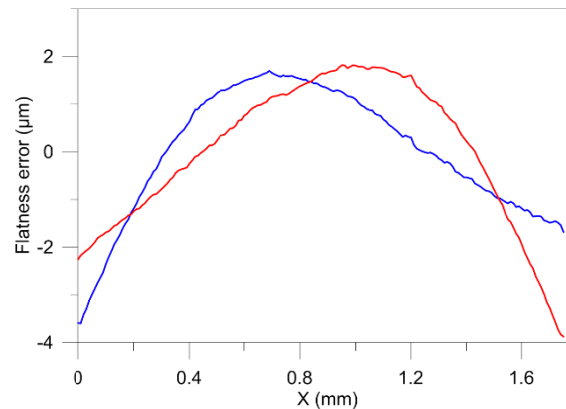


Figure 3. Residual flatness error for opposite slopes taken with a 10X objective on a Microdisplay Scan Confocal Microscope. Blue curve for 4.5 degrees, red curve -4.5 degrees.

This symmetry is normal to happen, since the flatness error is caused by the field curvature aberration, which has symmetry of revolution along the axis of the optical system. On a tilted profile, the left side from its center (optical axis will be nearly on the center) has a certain tilt angle pointing to the center, while the right side has the inversed tilt angle.

The same behavior is observed when the same steps are performed in the Y direction: a Y profile crossing the optical axis of a tilted surface on the Y direction equals an X profile of a tilted surface on the X direction for the same tilted angle. Thus, characterizing one tilt direction will allow an extrapolation to the full flatness error by adjusting the tilt in the radial direction and the distance to the optical center.

Considering that the aberration depends not only on the tilt angle but also the distance from the optical center, a straightforward procedure to determine the optical center is proposed:

1. Measure two times a flat mirror with two different tilts in the X direction. Remove the dominant plane of each topography and subtract one topography to the other.
2. Extract the Y profile, perpendicular to the tilt direction, with the lowest peak-to-valley.
3. Repeat steps 1 and 2 with a tilted mirror in the Y direction, using the profile with the lower peak-to-valley along the X direction.
4. The intersection of these two profiles determines the optical center.

Figure 4 shows the aforementioned method. Fig. 4a shows the subtraction of two topographies taken at 0 and 6 degree tilts on the X direction with a 10X objective on a Microdisplay Scan Confocal Microscope, while Fig. 4b is the equivalent with a perpendicular tilt. Fig. 4c shows a series of profiles extracted column by column from Fig. 4a.

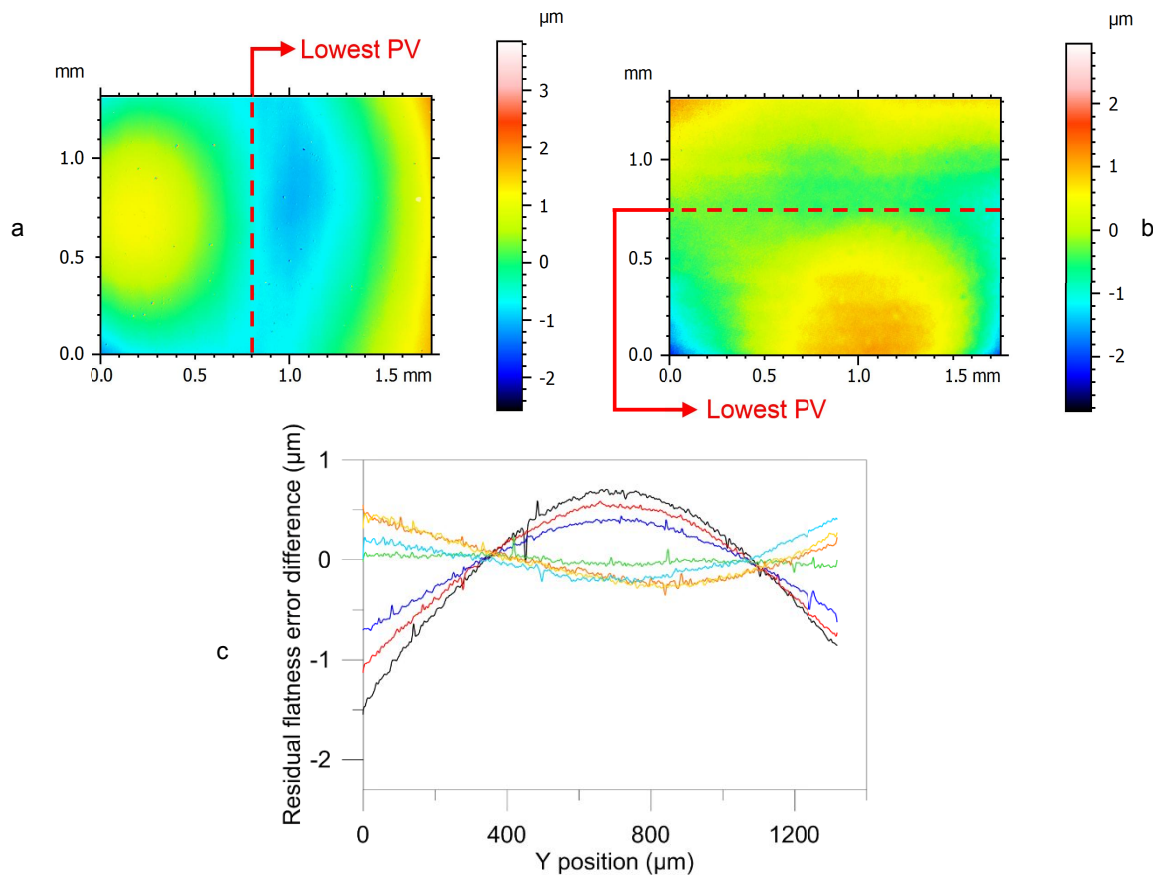


Figure 4. Subtraction of the residual flatness error of 6° and 0° tilted mirror in the (a) X direction and (b) Y direction. (c) Y profiles in different positions of X; an arbitrary offset has been applied so the peak-to-valley is more evident. The green line shows the profile that crosses the optical center.

The fact that the profile with lowest peak to valley is the one crossing the optical axis is straightforward to explain: for all the points crossing such profile, the slope pointing to the optical axis is zero, and since this topography has the 0 degree topography already subtracted, such profile must be totally flat. Any other point located outside of this profile will have a slope pointing to the optical axis different to zero, and thus a non-zero flatness error.

2.2 Construction of the flatness error model as a function of tilt angle and distance

The characterization of the residual flatness error of different slopes is made by fitting the error as a function of the distance to the optical center and the tilt angle. A tilted mirror in the X direction is measured from 0° to 10° for a 10X objective every 1 degree. For each topography, the profile crossing the optical axis and parallel to the tilt direction is extracted. The first and last point of the profile are used to measure its slope, and we remove such slope. Only positive slopes are measured due to the radial symmetry: the right half part of the profile of a positive slope is equivalent to the left half profile if measured with inversed tilt, and mirroring the profile with respect to the optical center. We split the obtained profile in the optical center into two halves and set the optical center as the origin. The right half will correspond to the positive slope, after mirroring in X, and the left half will correspond directly to the negative slope.

Figure 5 shows the three-dimensional surface constructed using the previous method. This topography allows us to extract the residual flatness error as a function of the radial slope and the distance to the optical center.

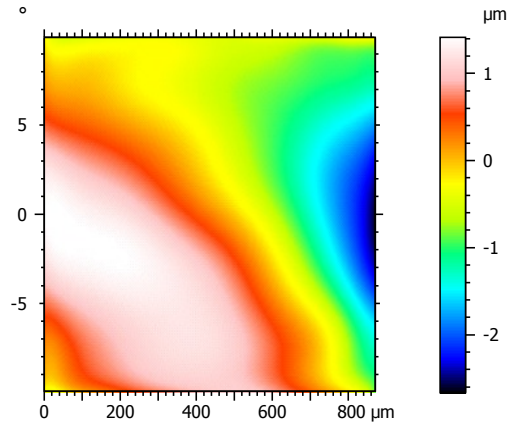


Figure 5. Residual flatness error surface build from the profiles of all angles measured. X axis is the distance to the optical center (μm), Y axis corresponds to the tilt angle (degrees) and Z axis is the residual flatness error (μm).

Using a mathematical fitting program, Systat Software Inc. TableCurve 3D, two different functions are proposed to fit the flatness error surface. We have chosen a 3rd order polynomial because of its computational simplicity and an 8th order Chebyshev polynomial because of its higher regression coefficient. Figure 6 shows the residuals of each polynomial with respect to the original surface in Figure 5 and as stated, the Chebyshev has lower error amplitudes.

The Chebyshev polynomial presents a drawback: it is not able to correct those points on the topography that has larger distances to the optical axis than the distances that are characterized. These are those points at the corners and the reason why this is happening is because of mathematical limitations of the Chebyshev function:

$$f(x, \alpha) = \sum_n \sum_m c_{n,m} T_n(x) T_m(\alpha) \quad (1)$$

with $c_{n,m}$ as the coefficient for each term, and

$$T_n(x) = \cos(n \arccos(x)) \quad (2)$$

where the x values are normalized to the interval $[-1,1]$ from the original data. Because of the presence of the arccosine function, the error calculation is limited to the region where the radial distance is equal or smaller than the characterized profile maximum distance. This causes those points of the topography with larger distances not to have correction values.

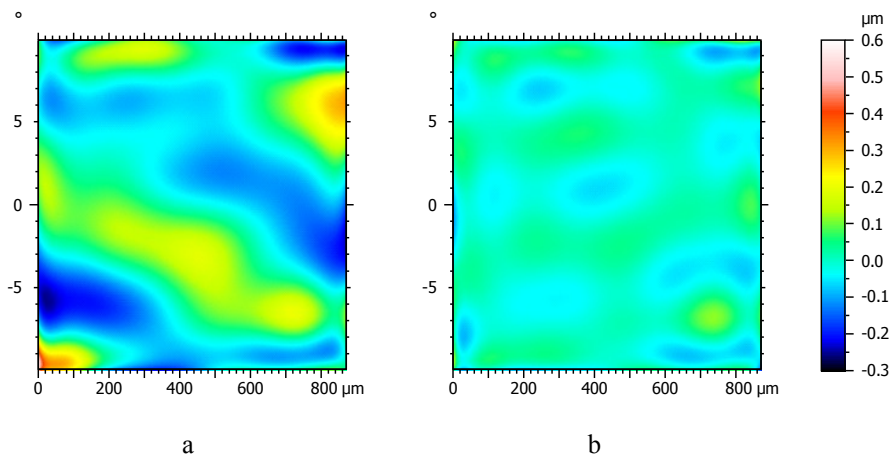


Figure 6. Differences between the measured profile and: (a) the 3rd order polynomial and (b) the 8th order Chebyshev polynomial.

2.3 Local slope calculation and flatness error correction

The correction polynomials will be applied to each point of the topography depending on the distance and the slope of such point towards the optical center (OC). Figure 7 shows the calculation of the derivative Dr of a point P towards the optical center. For such calculation, the derivatives Dx and Dy of the topography are calculated with a Savitzky-Golay polynomial method that is using a 5x5 pixel window. This ensures that the local slopes are only evaluated for the low frequency components of the surface, avoiding microscopic variations that typically can generate very large slope variations not responsible for the flatness error. The radial derivative Dr is finally calculated as the addition of the projected derivatives Dxr and Dyr along the direction of the optical axis.

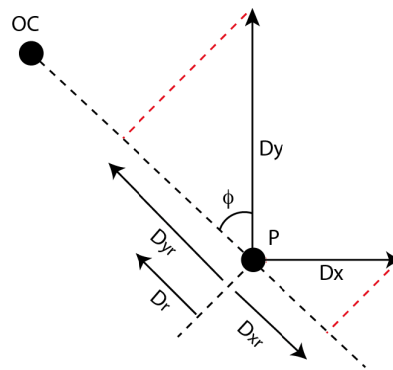


Figure 7. Calculation of the radial derivative Dr of any point P respect to the optical center OC . The angle ϕ defines the radial direction. Dx and Dy are the derivatives of the topography in the X and Y directions. The radial derivative is the addition of the projected derivatives Dxr and Dyr along the direction to the OC .

2.4 Optimized method

The method described in 2.2 has an inherent offset error: the leveling process that is allowing us to separate the flatness error from the global tilt of the surface is placing each new profile centered to zero in the Z axis. An optimized version of the calibration method is proposed to take this effect into account. We propose to measure a calibrated sphere with very low form error. Because a sphere contains a continuous slope variation, our proposed method should in principle correct the flatness error in a continuous way and leave a flat residual after the subtraction of a theoretical sphere with the calibrated radius. The reality is that the reference correction surface depicted in 2.2 is leaving a secondary residual topography coming from the centration of the original profiles. We average this secondary residual error for the pixels that present the same tilt and plot the error against the slope. The outcome is an offset function that has to be added to the correction surface. Figure 8 shows the offset correction curve that is evaluated on a 10.00 mm diameter reference sphere measured with a 10X objective on a Microdisplay Scan Confocal Microscope.

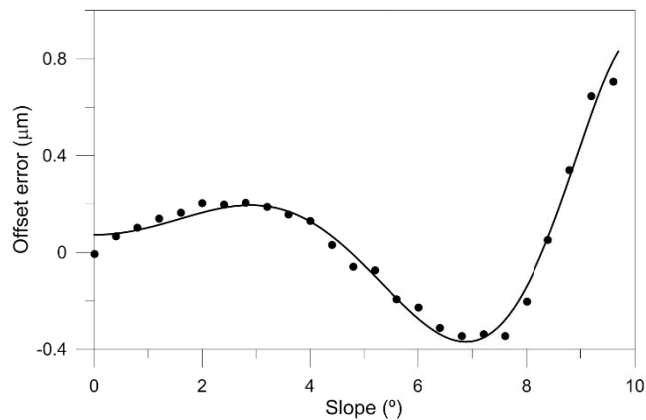


Figure 8: Offset values calculated from a 10.0 mm sphere with a 10X objective.

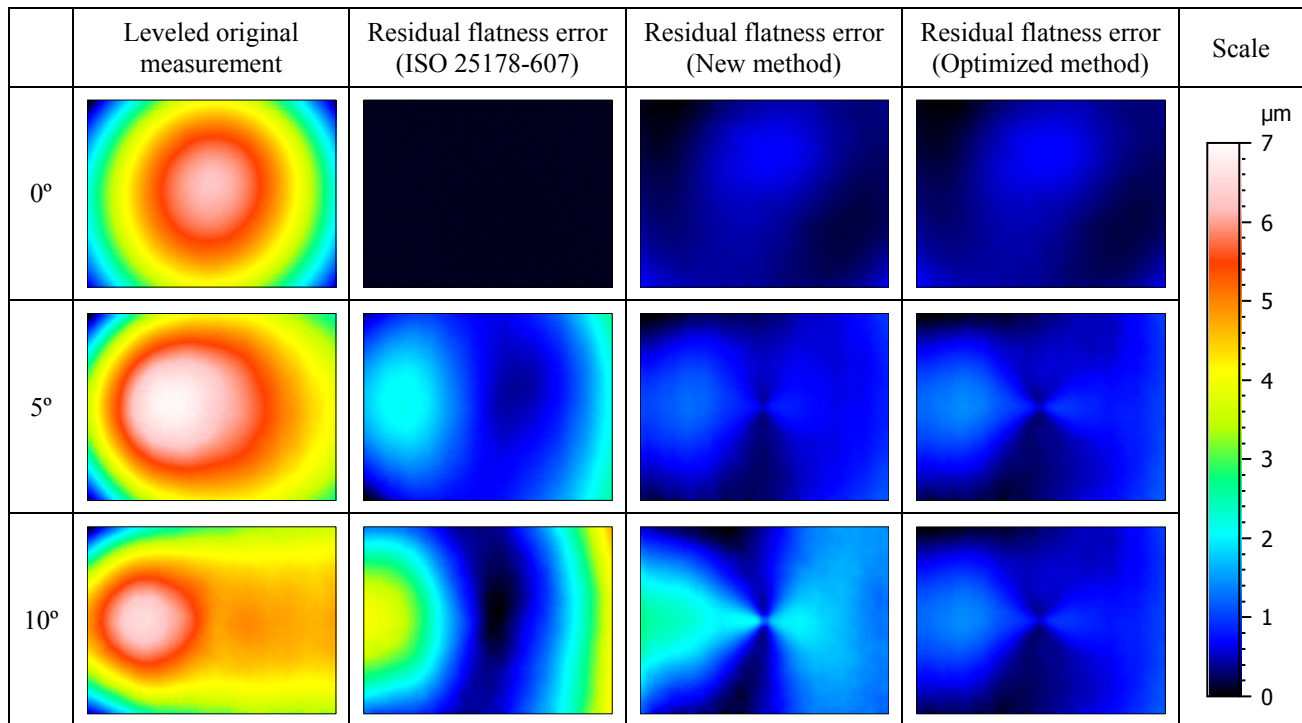
3. RESULTS AND DISCUSSION

In this section, we will compare the residual flatness error of the original measurement, the calibration method described in the ISO 25178-607, our proposed method and the optimized method for different surfaces. We will analyze a flat mirror tilted with different slopes, a sphere and finally a cylinder. All measurements are made using a 10X magnification objective on a Microdisplay Scan Confocal Microscope using a green LED with $\lambda = 0.550 \mu\text{m}$.

3.1 Mirror

A flat mirror is measured with different tilts, and then the dominant plane is removed from the surface to obtain the residual flatness error, and it is compared to the different calibration methods. Table 2 shows how the original residual flatness error is deformed when a tilt is applied, but it does not add amplitude to the maximum error. As expected, ISO 25178-607 produces a Gaussian noise as error when the surface is totally flat and leveled, but a form appears when the tilt angle increases. Our proposed methods produce a low amplitude error with flat and leveled surfaces and, although they increase in amplitude with the tilt, they do it less than the ISO 25178-607 method does, specially the optimized one.

Table 2. Residual flatness error of a flat mirror with different tilt slopes and each method for the aberration correction.



We have also studied the surface parameter S_z for the tilted flat mirror every 1°. The results are plotted in Figure 9, where we can check that the proposed method is better for correcting the residual flatness error of flat surfaces if they have a tilt of more than 2°, and the optimized method does not present significant improvements respect to the new method. In any case all methods correct substantially the flatness error.

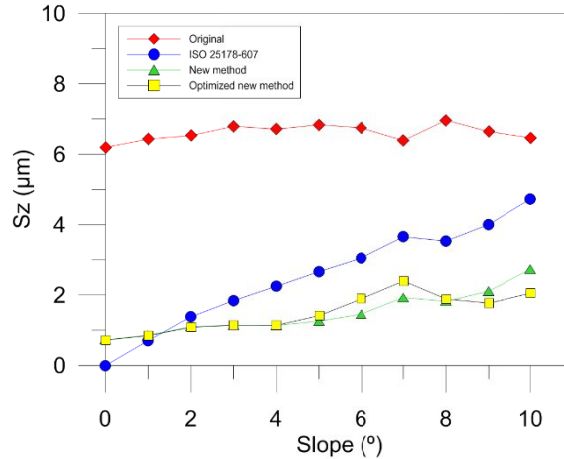


Figure 9. Sz values versus tilt angle for the 4 methods shown in Table 2.

3.2 Sphere

A calibrated sphere of 10.00 mm diameter with low form error has been measured with a 10X objective. Table 3 shows the values of the radius of curvature obtained after a best fit sphere, while Figure 10 is showing the residual flatness error topography. The errors are very similar in shape and peak to valley, but there is a substantial improvement in the evaluation of the radius of curvature that improves from 4% error in the case of the conventional calibration method down to 0.02% with the optimized method and the use of Chebyshev polynomial model. The main drawback is not being able to correct those points that are further away than the maximum characterized radius. This drawback can be avoided with a different strategy of flatness error characterization, such as tilting the reference mirrors along the profile that connects the corners of the camera, or by rotating the camera with a reference grid to the tilt angle direction, or any other strategy that is allowing to measure larger profiles than the ones used in this paper. The use of 3rd order polynomial extends the measurable field of view, at the expense of extrapolating the evaluation at further distance that has not been characterized, and with much larger residuals than the Chebyshev method. The 3rd order polynomial leaves a 2% error on the radius of curvature. Additionally, a sphere could contain larger local slopes than those characterized.

Table 3. Radius of a best fit sphere applied on a measured sphere of calibrated radius of 5.000 mm.

	Original	ISO 25718-607	New method	Optimized method
3 rd order polynomial	4.9453 mm	5.2055 mm	5.1027 mm	5.1049 mm
Chebyshev polynomial			5.0263 mm	4.9988 mm

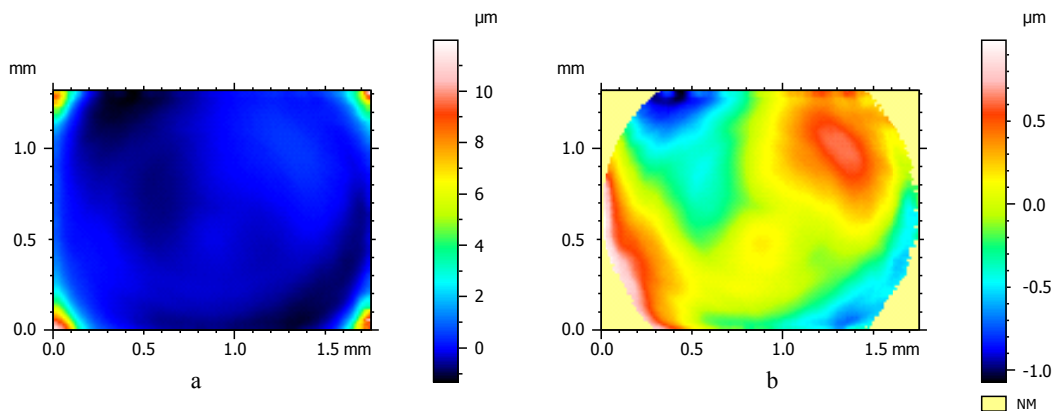


Figure 10. Residuals of removing a theoretical sphere with a radius of 5.000 mm using the optimized new method (a) with a 3rd order polynomial, (b) an 8th order Chebyshev.

3.3 Cylinder

A calibrated reference rod (Mahr ref. 4828118, $\text{Ø}10.000 \pm 0.001$ mm) has been measured with a 10X objective with the cylinder axis parallel to the X direction and the correction method applied. Figure 11 shows the residual flatness error for both, the 3rd order and the Chebyshev polynomials. Both methods provide similar results. For a cylinder sample, it has to be noted that the profile parallel to the X direction on top of the cylinder has no local slope, while the Y profiles are equal circles, but with local slopes towards the optical center different from the local slope of the circle itself.

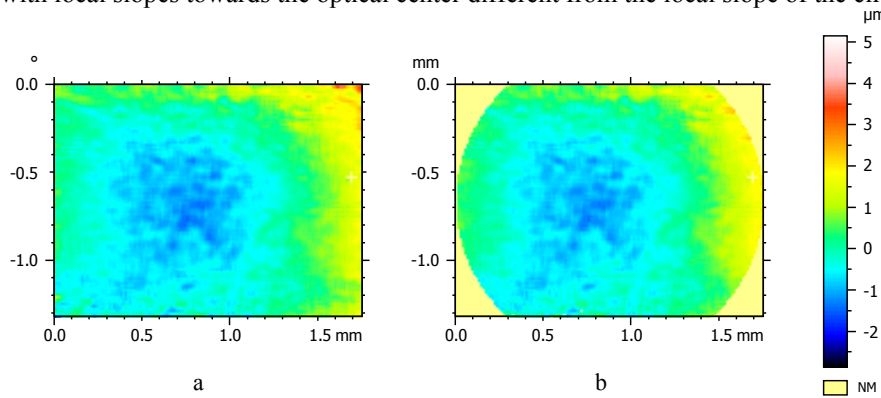


Figure 11. Residuals of removing a theoretical cylinder with a radius of 5.000 mm using the optimized new method with (a) a 3rd order polynomial, or (b) an 8th order Chebyshev.

4. CONCLUSIONS

In this paper, we have shown that confocal microscope profilers (Laser Scan and Microdisplay Scan) have a flatness deviation error that changes in shape with the tilt of the surface. The accepted method to calibrate the flatness error described in the ISO 25178-607 is valid for flat surfaces placed perpendicular to the optical axis of the system, but fails for tilted surfaces with increasing errors up to few micron PV for a 10X objective. We have proposed a calibration methodology that characterizes the flatness error dependence on the distance to the optical axis and on the slope of the surface by measuring a set of topographies of a mirror at varying tilt angles. Two different error corrections based on 3rd order polynomial and Chebyshev polynomials have been studied, the latter providing better results but with limited field of view. The method, applied to a flat surface tilted up to 10 degrees showed an improvement from 6 to 2 μm PV, to a calibrated sphere provided a radius of curvature measurement with less than 0.05% error.

Future work will be needed to extend the proposed calibration method for different magnification objectives, and larger tilt values. It will be also needed to investigate a method to characterize the error at distances longer than the field of view of the camera, allowing the Chebyshev polynomials to be applied to all points of the topography. We also foresee further investigation of the Petzval aberration simulation using a real microscope objective optical design.

REFERENCES

- [1] Leach R. "Optical Measurement of Surface Topography," Springer Verlag ISBN 978-3-642-12012-1
- [2] ISO 25178, Geometrical product specifications (GPS) — Surface texture: Areal — Part 607: Nominal characteristics of non-contact (confocal microscopy) instruments
- [3] Giusca, C., Leach, R. "Calibration of the scales of areal surface topography-measuring instruments: part 1. Measurement noise and residual flatness," Measurement Science and Technology (2012).
- [4] Matilla, A., Bermudez, C., Mariné, J., Martínez, D., Cadevall, C., and Artigas, R. "Confocal unrolled areal measurements of cylindrical surfaces," Proc. SPIE 10329, Optical Measurement Systems for Industrial Inspection X, 1032915, doi: 10.1117/12.2269631 (2017)
- [5] Sensofar Tech App. Note. "Flatness error on Imaging Confocal Microscopes," 20 February 2009, <http://www.sensofar.com/references/FlatnessError.pdf> (11 April 2017).
- [6] Su, R., Wang, Y., Coupland, J., Leach, R. "On tilt and curvature dependent errors and the calibration of coherence scanning interferometry," Optics Express 25(4), 3297-3310 (2017)